

# Simulation of Optical Dot Gain in Multichromatic Tone Production

Li Yang, Sasan Gooran and Björn Kruse

Institute of Science and Technology, Linköping University, Norrköping, Sweden

Optical dot gain (light scattering or Yule–Nielsen effect) is an important effect influencing the quality of tone reproductions. Based on probability descriptions on the light scattering, a framework is established for describing this effect on the reflectance and color appearance of a chromatic halftone image. General expressions for the reflectance and CIEXYZ tristimulus values have been derived. Simulations for images printed with 2 inks have been carried out by applying Gaussian type of point spread function (PSF). Dependence of the optical dot gain on the optical properties of substrate and inks, the dot geometry etc., have been studied in detail.

Journal of Imaging Science and Technology 45: 198–204 (2001)

## Introduction

Optical dot gain refers to the fact that a printed dot appears bigger than it geometrically is. It is because light that enters the substrate under the dot can exit from the substrate between dots due to light scattering in the substrate. It was Yule and Nielsen<sup>1</sup> who first interpreted the phenomenon and proposed a semi-empirical modification to the simple Murray–Davies equation.<sup>2</sup> Because of this optical dot gain is also called Yule–Nielsen effect. The optical dot gain depends on the optical properties of the materials (paper, ink) and geometrical distribution of ink dots (resolution, location, size and shape). To account for the optical dot gain is practically important in graphic arts and has long been an interesting topic of research in theoretical, simulation and experimental perspectives.<sup>1,3–14</sup> However, so far the studies have mainly been focused on monolayer color printing processes. Little has been done for the multi-layer case. Because the multichromatic halftone images consist of two or more inks which form many distinct chromatic regions, the behavior of Yule–Nielsen effect becomes complicated and consequently the analysis becomes very difficult if no theoretical model serves as a guide.

This article contains the following parts. First a framework that accounts for the effects of optical dot gain in multi-chromatic tone reproduction is worked out. Then the present approach is illustrated by applying it to some examples. Finally discussions about optical dot gain in optical and chromatic perspectives are given.

## A Model for Multichromatic Tone Reproduction

A chromatic halftone image usually consists of 3 or more inks, which form many distinct color regions covered by none, one or a few ink layers. We start our study from an image printed with 2 inks and then generalize the framework to an image consisting of any number of

inks. In this study, we have assumed that there is no ink penetration, because as we have shown optically ink penetration can be equally described by introducing an extra ink layer while the substrate remains clean.<sup>15</sup> Therefore all equations we work out here can directly be applied to the case where there exists ink penetration as long as the transmittance is replaced by *combined transmittance* which is a collective property the ink and the paper.

## Image Printed with Two Inks

Figure 1 is a side view of an image printed with two inks. The transmittances of the ink layers are,  $T_I$  and  $T_{II}$ , respectively. The image can be divided into 4 distinct chromatic regions, denoted as  $\Sigma_0$  through  $\Sigma_3$ , which correspond to white ( $\Sigma_0$ ), primary ( $\Sigma_1, \Sigma_3$ ) and secondary ( $\Sigma_2$ ) color, respectively. If the tonal values of the two inks are  $a$  and  $b$ , the area of the  $i$ th chromatic region,  $\sigma_i$ , depends on the model of color mixture adopted by the printer. For example, when the ink dots are placed at random,  $\sigma_i$  can be computed by

$$\begin{aligned} \sigma_0 &= (1 - a)(1 - b) \\ \sigma_1 &= a(1 - b) \\ \sigma_2 &= ab \\ \sigma_3 &= (1 - a)b \end{aligned} \tag{1}$$

Similarly to the monolayer case,<sup>14</sup> we define  $P_{ij}$  as probability that a photon exits the substrate from  $\Sigma_j$  if it

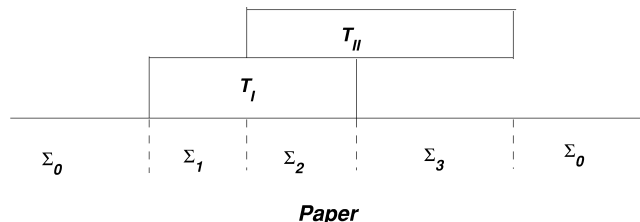


Figure 1. A side view of a multilayer halftone image.

Original manuscript received October 10, 2000

©2001, IS&T—The Society for Imaging Science and Technology

enters the substrate at  $\Sigma_i$ . If the image is uniformly illuminated by light of intensity  $I_0$  the outgoing flux of the light from  $\Sigma_j$  due to scattering of the incident light at  $\Sigma_i$  may be written as,

$$J_{ij} = I_0 T_i T_j P_{ij} \sigma_i \quad (i, j = 0, \dots, 3) \quad (2)$$

where  $T_i$  is the combined transmittance values describing the transmittance of the ink layer(s) and ink penetration of the region  $\Sigma_i$ , for example,  $T_0 = 1$ ,  $T_1 = \tau_I$ , ( $T_3 = T_{II}$ ) and  $T_2 = T_I T_{II}$ . Similar to the monolayer system,<sup>14</sup> it is easy to show that the probabilities  $P_{ij}$  ( $j = 0-3$ ) are constrained by the reflectance of the substrate, i.e.,

$$\sum_{j=0}^3 P_{ij} = R_g \quad (i = 0, \dots, 3) \quad (3)$$

In addition, the probability  $P_{ij}$  and its counterpart  $P_{ji}$  fulfil the following correlation relation,

$$P_{ij} \sigma_i = P_{ji} \sigma_j \quad (i, j = 0, \dots, 3) \quad (4)$$

Due to light scattering, photons enter the substrate at  $\Sigma_i$  can exit from  $\Sigma_j$ . Thus the total flux of the light outgoing from  $\Sigma_j$  may be expressed as

$$J_j = \sum_{i=0}^3 J_{ij} = \sum_{i=0}^3 I_0 T_i T_j P_{ij} \sigma_i \quad (j = 0, \dots, 3). \quad (5)$$

Applying the constraint conditions and the correlation (Eqs. 3 and 4), one can further write the flux as

$$J_i = I_0 T_j^2 R_g \sigma_j - I_0 \sum_{i=0, i \neq j}^3 T_j (T_j - T_i) P_{ji} \sigma_j \quad (j = 0, \dots, 3) \quad (6)$$

Accordingly the reflectance of the  $\Sigma_j$  region is calculated by

$$R_j = T_j^2 R_g \sum_{i=0, i \neq j}^3 T_j (T_j - T_i) P_{ji} \quad (j = 0, \dots, 3) \quad (7)$$

Thus the regional reflectance  $R_j$  depends directly on the transmittance ( $T_j$ ) of the ink layer. It depends also on differences of the transmittances between the incident and exit regions, ( $T_j - T_i$ ), and the probability of the light transfer between the two regions, ( $P_{ji}$ ).

Knowing the reflectance,  $R_j$ , one can further calculate the average reflectance of the image, by

$$\begin{aligned} R &= \sum_{j=0}^3 R_j \sigma_j \\ &= \sum_{j=0}^3 T_j^2 R_g \sigma_j - \sum_{j=0}^3 \sum_{i \neq j}^3 T_j (T_j - T_i) P_{ji} \sigma_j \\ &= \sum_{j=0}^3 T_j^2 R_g \sigma_j - \sum_{j=0}^3 \sum_{i < j} (T_i - T_j)^2 P_{ji} \sigma_j \end{aligned} \quad (8)$$

where the first term is the reflectance of the halftone image under the Murray–Davies assumption, and the second is due to the light scattering.

### Image Printed with Multiple Inks

The framework established above can be directly generalized to a printed image involving many inks. If the image consists of  $N$  distinct chromatic regions, ( $N \leq 8$  or 16, for images containing 3 or 4 inks, respectively),

the regional reflectance of the region  $\Sigma_j$  can be computed by

$$R_j = T_j^2 R_g - \sum_{i=0, i \neq j}^{N-1} T_j (T_j - T_i) P_{ji} \quad (j = 0, \dots, N-1) \quad (9)$$

The overall reflectance of the whole image is given by

$$R = R_{MD} - \Delta R \quad (10)$$

where

$$R_{MD} = \sum_{j=0}^{N-1} T_j^2 R_g \sigma_j \quad (11)$$

is the reflectance of the halftone image under Murray–Davis assumption, and

$$\Delta R = \sum_{j=0}^{N-1} \sum_{i < j} (T_i - T_j)^2 P_{ji} \sigma_j \quad (12)$$

is a term corresponding to the so called Yule–Nielsen effect or optical dot gain. From these one can draw the conclusion that optical dot gain is a general phenomenon in multichromatic tone reproduction. Because  $\Delta R$  is a non-negative quantity, Eq. 10 means that the real reflectance of the halftone image,  $R$ , is smaller than that predicted by applying Murray–Davies assumption.

It is worth to notice that it is not the ink dots but the distinct chromatic regions that are directly related with the color appearance of the image. Therefore the term for optical dot gain becomes no longer intuitively clear as it was for monochromatic case, because the distinct regions are not necessarily bigger optically than they are geometrically. For example, due to light scattering from  $\Sigma_1$  into  $\Sigma_0$ ,  $\Sigma_1$  appears to be extended towards  $\Sigma_0$  along  $\Sigma_0/\Sigma_1$  border (see Fig. 1). However  $\Sigma_1$  appears to be compressed due to the light scattering from  $\Sigma_2$  into  $\Sigma_1$  (i.e., the region of  $\Sigma_1$  close to  $\Sigma_2$  appears as if it is of the secondary color). The total effect of the light scattering on the regional reflectance of  $\Sigma_1$ ,  $R_1$ , is a combination of these opposite contributions. This is why the term  $(T_j - T_i)$  comes into Eq. 9. Therefore the term for optical dot gain should refer to the image as whole rather than any individual chromatic region.

### Simulation of Multilayer Color Image

The model presented above shows that all the regional reflectance values,  $R_j$ , the overall reflectance value of the image,  $R$ , and the corresponding optical dot gain,  $\Delta R$ , depend on a set of independent probabilities  $P_{ij}$  which is  $N(N-1)/2$  in number, where  $N$  is the number of the distinct color regions. For example, in two inks case there are 6 independent probabilities,  $P_{01}, P_{02}, P_{03}, P_{12}, P_{13}$  and  $P_{23}$ .

As defined in Eq. 2,  $J_{ij}$  represents the flux of light that enters the substrate in the region,  $\Sigma_i$ , and then is scattered into  $\Sigma_j$ . By the definition of the point spread function,  $J_{ij}$  can also be written as,

$$J_{ij} = I_0 T_i T_j \int_{\Sigma_i} \int_{\Sigma_j} p(x_i - x_j, y_i - y_j) d\sigma_i d\sigma_j \quad (13)$$

Comparing Eq. 2 with Eq. 13 one gets

$$P_{ij} = \frac{1}{\sigma_i} \int_{\Sigma_i} \int_{\Sigma_j} p(x_i - x_j, y_i - y_j) d\sigma_i d\sigma_j \quad (14)$$

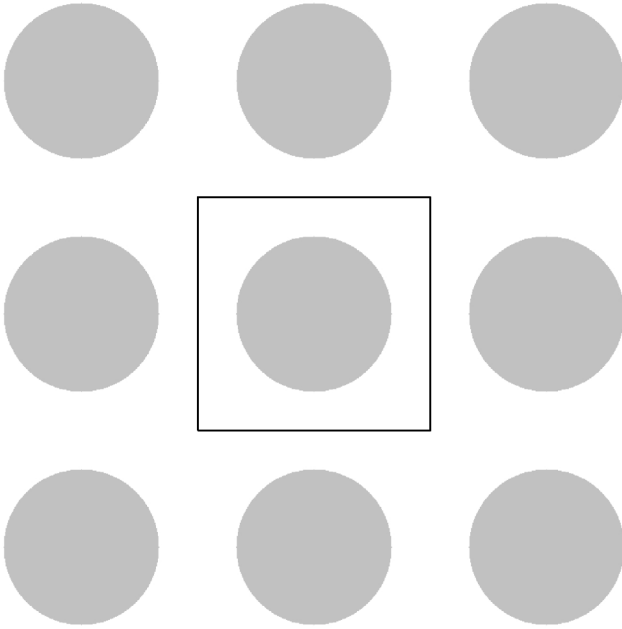


**Figure 2.** A mask contains 3 halftone cells. Contributions from the neighbor dots to the center one are included in convolution (see Eq. 14).

**TABLE I. Transmittance of Distinct Chromatic Regions**

Regions	$\Sigma_0$	$\Sigma_1(\Sigma_3)$	$\Sigma_2$
Transmittance	1	$T_i(T_{ii})$	$T_i T_{ii}$

Because the PSF is closely related to the optical properties of the substrate, the quantity  $P_{ij}$  depends on these properties as well. For example, if the PSF is Gaussian,

$$p(x_i - x_j, y_i - y_j) = \kappa e^{-[(x_i - x_j)^2 + (y_i - y_j)^2] / \delta^2} \quad (15)$$

the optical properties of the substrate is characterized by the Gaussian parameter  $\delta$  ( $\kappa$  is a factor of normalization). This kind of PSF has been proven to fit the experimental data of Yule and co-workers quite well.<sup>4,16</sup> Because variables of the PSF,  $(x_i - x_j)$  and  $(y_i - y_j)$ , are related with the relative position between regions  $\Sigma_i$  and  $\Sigma_j$ ,  $P_{ij}$  depends on the spatial distribution of the printed ink dots. Furthermore the integrated value,  $P_{ij}$ , depends on the size and shape of the integration areas ( $\Sigma_i$  and  $\Sigma_j$ ). Finally the magnitude of optical dot gain depends on the combined transmittance values of related regions and their difference,  $(T_i - T_j)^2$ , as can clearly be seen from Eq. 12. To examine to what extent these factors affect the computed reflectance values, simulations have been carried out by applying Gaussian type of point spread function to images printed with two inks.

### Two Inks Printed with Round Dots

For simplicity, we first assume that the ink dots are coaxial in position (dot on dot) and round in shape. The simulations are carried out by choosing a mask that contains  $3 \times 3$  halftone dot cells (see Fig. 2), therefore influences to the convolution (Eq. 14) from the

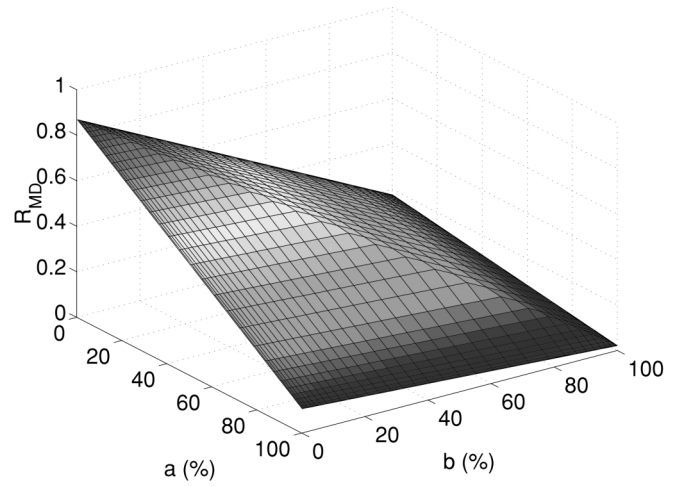


**Figure 3.** Computed  $R_{MD}$ , two inks, dot on dot,  $R_g = 0.87$ ,  $T_i = 0.35$ ,  $T_{ii} = 0.45$ .

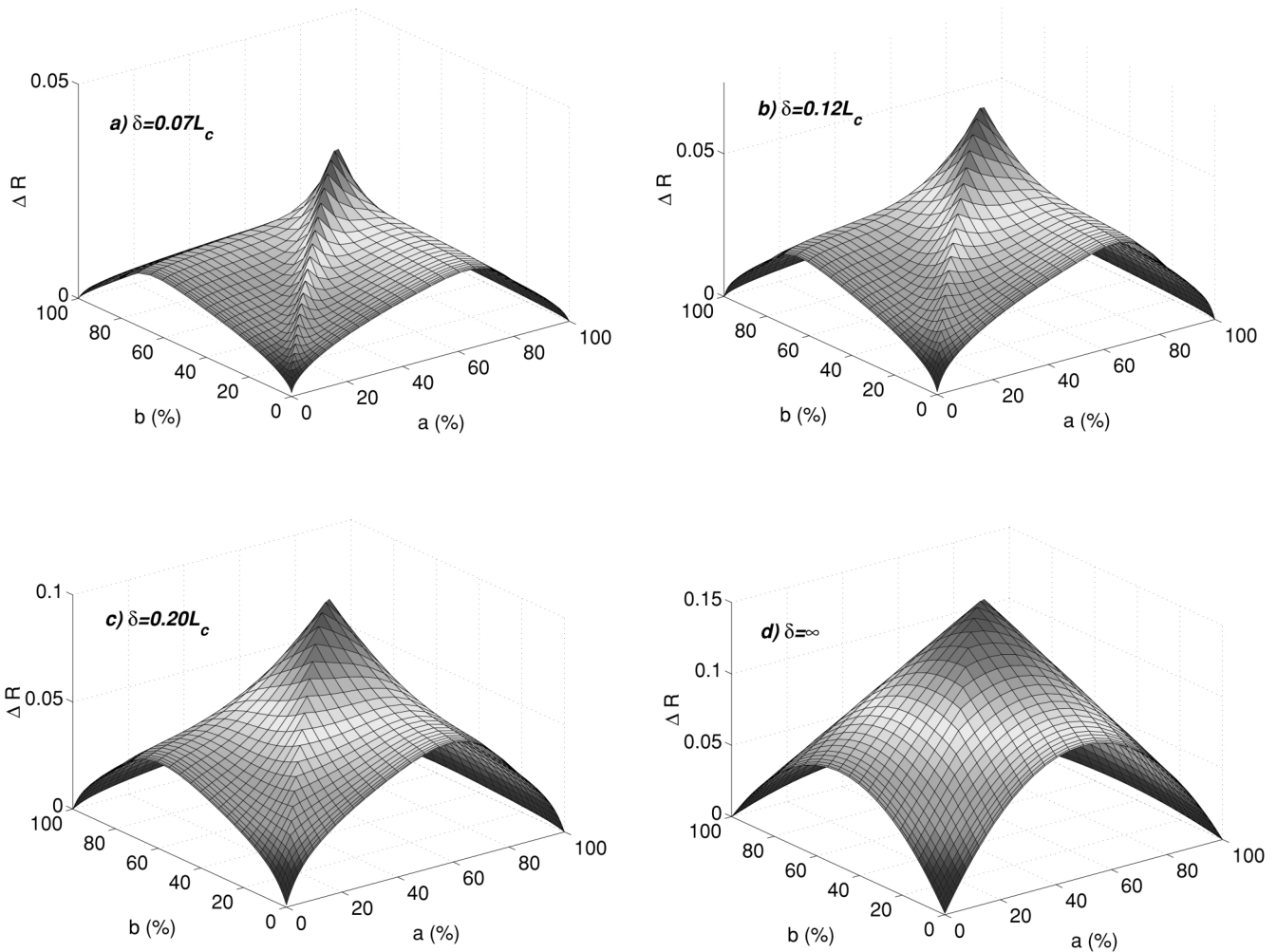
nearest neighbor dots have been included. Fig. 3 and 4 are the demonstrations of computed reflectance value ( $R_{MD}$ ) under Murray–Davies assumption and optical dot gain ( $\Delta R$ ). The printed image consists of four ink spots, white, two primary colors (substrate covered by either ink 1 or 2) and one secondary color. The transmittance values corresponding to these regions are collected in Table I. Because the reflectance value computed according to Murray–Davies model,  $R_{MD}$ , is a bi-linear function of the tonal values,  $a$  and  $b$ , it has a roof like structure with maximum along the line  $a = b$  (see Fig. 3).

Figure 4 presents the computed  $\Delta R$  with respect to different values of Gaussian parameter,  $\delta$ . For generality, the length (or width) of a halftone cell,  $L_c$ , has been chosen as a unit (ruler) of the parameter  $\delta$ . Figures 4a through 4c correspond to  $\delta = 0.07L_c$ ,  $0.12L_c$  and  $0.20L_c$ , respectively. An extreme case,  $\delta = \infty$ , is given in Fig. 4d) as well. The following facts are observed,

1.  $\Delta R$  has local maxima when the printed dots have identical sizes,  $a = b$  (ie. they completely overlap with each other).
2. The local maxima become wider and therefore less prominent when the Gaussian parameter,  $\delta$ , gets bigger or equivalently the PSF becomes broader and more flat.
3. The magnitude of  $R$  becomes bigger when  $\delta$  is bigger (Observe that scales of the subfigures are different).

The appearance of the local maxima is a hybrid of the difference of the transmittance values between adjacent regions and the effective extension of the PSF in space. For simplicity of explanation, we assume that the area covered by ink 1 ( $\Sigma_1$ ) has a fixed radius,  $r_1$  (Fig. 5). Now we examine the process when the radius of the area covered by ink 2 ( $\Sigma_2$ ),  $r_2$ , increases from  $r_2 = 0$  through  $r_2 = r_1$ . From this viewing point, we are actually looking at a cross section of  $\Delta R$  surface cut by a plane, say  $a = constant$ . According to Eq. 12  $\Delta R$  consists of 3 terms,

$$\begin{aligned} \Delta R = & 2(1 - T_1)^2 P_{01} \sigma_0 \\ & + 2(T_1 - T_2)^2 P_{12} \sigma_1 \\ & + 2(1 - T_2)^2 P_{02} \sigma_0 \end{aligned} \quad (16)$$



**Figure 4.** Computed ( $\Delta R$ ) for different Gaussian parameters  $\delta$ , two inks, dot on dot,  $L_c$  the length (width) of a halftone cell.  $R_g = 0.87$ ,  $T_I = 0.35$ ,  $T_{II} = 0.45$ .

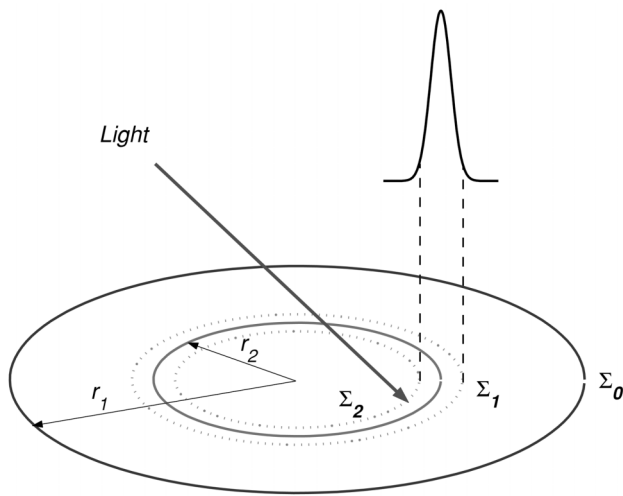


**Figure 5.** A systematic diagram for point spread function and dot geometry;  $L_c$  is the length (width) of the halftone cell.

Clearly, the first term comes from light scattering between regions  $\Sigma_0$  and  $\Sigma_1$ , the second term from that between  $\Sigma_1$  and  $\Sigma_2$  and third between  $\Sigma_0$  and  $\Sigma_2$ . Because we have assumed that  $r_1$  is fixed in the current consideration, the first term remains constant. Considering a photon that enters the substrate at  $(x, y)$  in  $\Sigma_2$  (region producing secondary color), the PSF that describes the probability of finding the photon at a point  $(x', y')$  becomes very small when

$$\sqrt[2]{(x-x')^2 + (y-y')^2} \geq 2\delta.$$

Therefore only when the photon strikes the substrate at a point in  $\Sigma_2$  close enough to the  $\Sigma_2/\Sigma_1$  border (inside the region marked by dot line circles), is there remarkable probability to find it in the adjacent region  $\Sigma_1$ . In the other words, the main contribution to the second term is from photons that hits the region between the dot line circles. At the same time, there is little chance for the photon to exit the substrate from the non-inked region ( $\Sigma_0$ ) i.e., the third term is negligible, if  $r_2 \ll r_1$  and  $d \ll |r_1 - r_2|$ . However the third term grows when  $r_2$  is approaching  $r_1$  (or  $a \rightarrow b$ ). Considering the fact that  $\Delta R$  is proportional to the quantity  $(T_i - T_j)^2$  (see Eq. 16 which has the biggest value in the third term

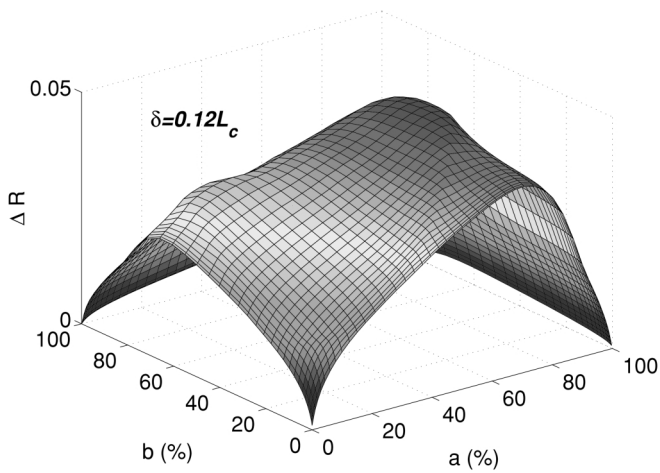


**Figure 6.** Computed  $\Delta R$  for two inks, dot off dot (separation of the dot centers =  $0.35L_c$ ), Gaussian parameter  $\delta = 0.12L_c$ ,  $R_g = 0.87$ ,  $T_I = 0.35$ ,  $T_{II} = 0.45$ .

(i.e.,  $(1 - T_1)^2 > (T_1 - T_2)^2$ ),  $\Delta R$  grows at a quicker pace when  $r_2$  is close to  $r_1$  ( $r_1 \rightarrow r_2$ ). After  $r_1 = r_2$ , however, if  $r_2$  continuously increases ( $r_2 \geq r_1$ ),  $\Delta R$  falls again. Thus  $\Delta R$  reaches its maximum when  $a = b$ . This explanation is consistent with that of fact No. 2. When  $\delta$  gets bigger, the PSF becomes broader and more flat. Correspondingly the area marked by the dot line circles becomes wider and therefore the local maxima of  $\Delta R$  become broader and (relatively) less prominent, although its absolute quantity increases. Because there is a higher probability that the photon enters the substrate in one region and exits from the other (or even others) in the case of having a large Gaussian parameter,  $\delta$ ,  $\Delta R$  becomes larger. An extreme case is when  $\delta \rightarrow \infty$ . In this case the PSF becomes constant ( $P_{ij}$  as well) over the whole paper. It means that the photon has an equal probability to be found anywhere on the paper, no matter where the photon enters the paper. Therefore the photon is said to be “completely scattered”.<sup>7</sup> Then the local maxima disappear and only a global maximum is built. As shown in the figures the location of the global maximum moves towards  $a = b = 50\%$  when the Gaussian parameter ( $\delta$ ) increases.

It is a common practice in the printing industry that the inks are not printed one on top of the other. Sometimes it is on purpose to avoid overlap as much as possible in order to achieve larger color gamut.<sup>17</sup> To simulate such a printed image, we set the centers of the dots (round dots) at different positions and then evaluate the optical dot gain regarding to the area of each dot. The simulation of the optical dot gain of such a system, is shown in Fig. 6. Because the dots are located at different positions, they have no overlap when they are small in size and the image consists of paper and primary colors only. After the dot sizes increase to some extent, these dots start overlapping and the secondary color emerges. Because the overlap depends on the size of the dots and the separation of dots' centers in space, the optical dot gain function has a complicated shape.

### Two Inks Print with Square Dots

To study the shape dependence of the printed dots (tonal values), simulations to images printed with square dots have also been carried out. Unlike the print

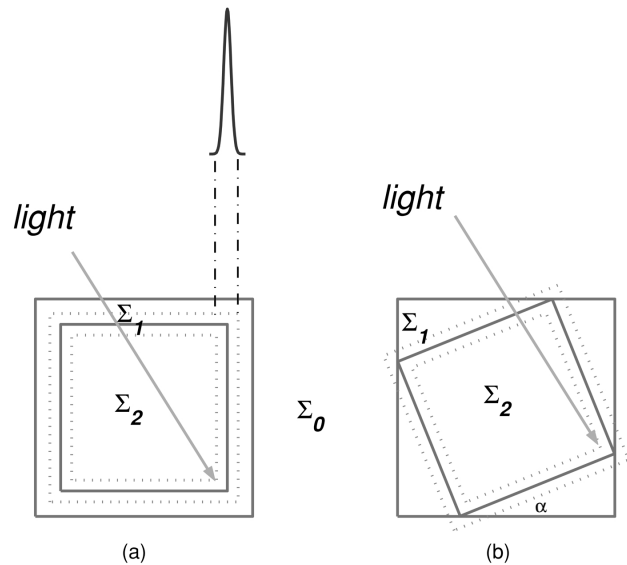


**Figure 7.** Two inks print, solid line squares represent two ink dots (areas  $a$  and  $b$ ).

with round dots, color appearance of the print with square dots depends not only on the areas of ink dots but also on the angles,  $\alpha$ , between the screen lines of the ink dots. Figure 7a is a prototype of the geometric formation for square dots, where each solid line square represents a square dot with area  $a$  or  $b$ . Figure 7b corresponds to the case where there is a screen angle between the dots. Naturally, to clarify the dependence of Yule–Nielsen effect ( $\Delta R$ ) on the dot shapes, comparisons will be made to images printed with round dots. For easier comparison, the identical Gaussian parameter,  $\delta = 0.12L_c$ , has been used in the simulations, where  $L_c$  is the length of a halftone cell as defined before. Furthermore dependence of Yule–Nielsen effect on the angle between the screen lines will also be explored, by choosing different  $\alpha$  values.

Figures 8a through 8d are the computed  $\Delta R$  corresponding to  $\alpha = 0^\circ$ ,  $15^\circ$ ,  $30^\circ$ , and  $45^\circ$ , respectively. Comparing this to the case of round dots (Fig. 4b), little difference has been observed when  $\alpha = 0$ . However  $\Delta R$  appears remarkably different when  $\alpha = 15^\circ$  and the differences become even bigger for bigger screen angle,  $\alpha$ . The differences can be summarized as

1. the local maxima along the diagonal  $a = b$ , which is prominent in the round dots case, becomes broader and much less evident.
2. the global maximum which is a sharp peak in the case of round dots becomes a broad plateau for the square dots case (where  $\alpha \neq 0$ ).

Because the point spread function has a limited effective extension (characterized by Gaussian parameter  $\delta$ , as shown in Fig. 7a), there is no significant probability for a photon to be scattered from one region (say  $\Sigma_2$ ) into another (say  $\Sigma_1$ ), unless the photon hits the substrate at a point close enough to the border of the incident region (marked by a dotted line square). In the case of  $\alpha = 0^\circ$ , there is little probability for the photon to transfer from  $\Sigma_2$  into  $\Sigma_0$  or vice versa,

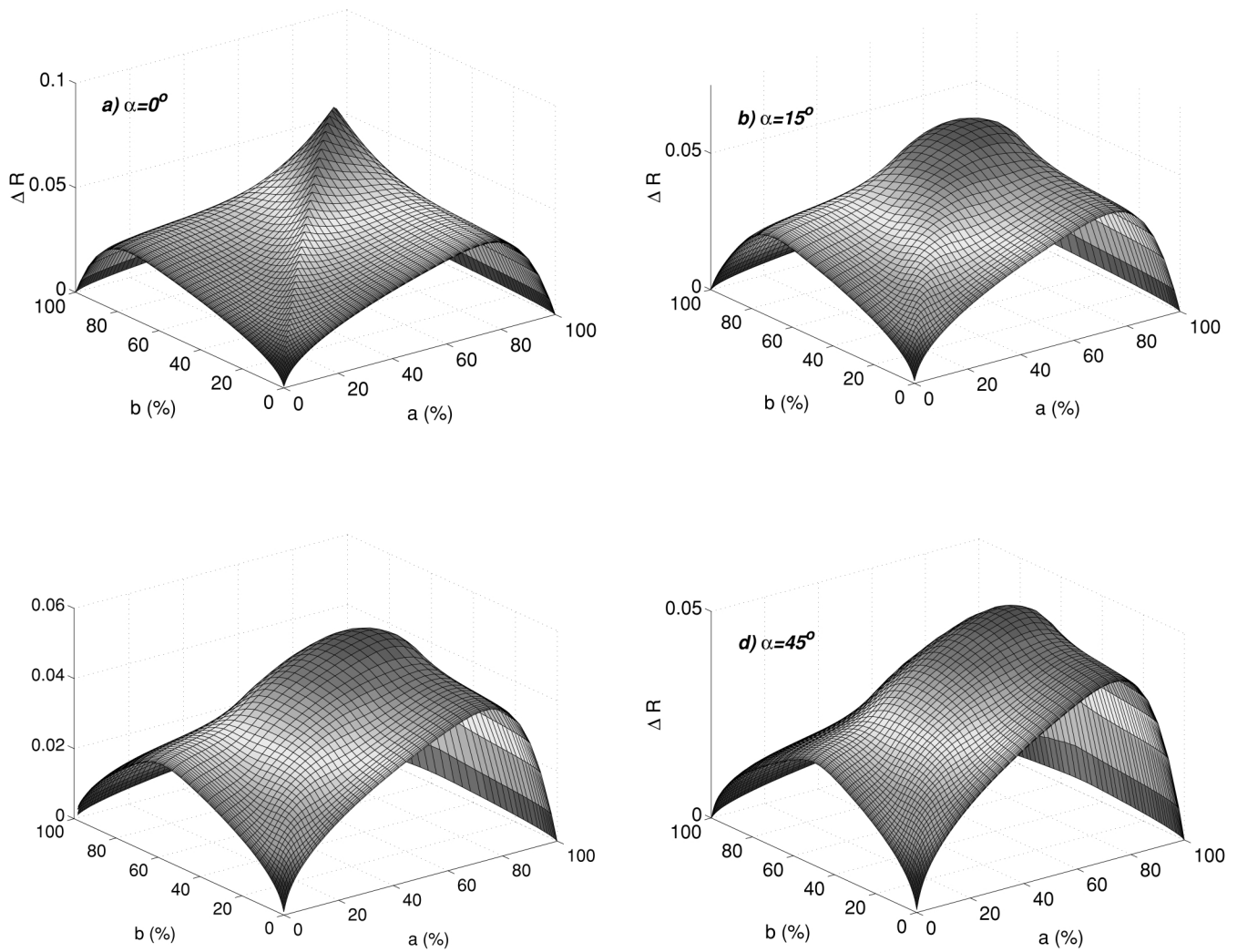


**Figure 8.** Computed ( $\Delta R$ ) for different screen angles,  $\alpha = 0^\circ, 15^\circ, 30^\circ, 45^\circ$ ,  $\delta = 0.12L_c$ , square dots (dot on dot).

if  $a \neq b$ . In other words, it happens only when the two ink dots have similar areas ( $b \approx a$ ). Correspondingly narrow local maxima appear along the diagonal  $a = b$ , as shown in Fig. 8a. However when  $\alpha \neq 0$ , if a photon strikes the substrate near a corner of the inner square, the photon has a better chance to be scattered from  $\Sigma_2$  into  $\Sigma_0$  or vice versa, even though the areas of the ink dots are not similar (see Fig. 7b). (Note that the rotated square has the same size as that in Fig. 7a) Therefore the local maxima become broader and more flat and therefore less prominent. This argument holds also for the broader appearance of the global maximum which appears to be a flat plateau. The simulations also show that the quantities of computed  $\Delta R$  decrease as the screen angle,  $\alpha$ , increases. Therefore increasing the screen angle may be helpful for reducing the optical dot gain.

### The Effects of Optical Dot Gain on Color Reproduction

The effects of optical dot gain on the color appearance of printed images can readily be seen from their tristimuli. According to definition, CIEXYZ tristimulus values can be computed as

$$\begin{aligned} X &= \int R(\lambda)S(\lambda)\bar{x}(\lambda)d\lambda \\ Y &= \int R(\lambda)S(\lambda)\bar{y}(\lambda)d\lambda \\ Z &= \int R(\lambda)S(\lambda)\bar{z}(\lambda)d\lambda \end{aligned} \quad (17)$$

where  $S(\lambda)$  is the energy distribution of the illumination and  $\bar{x}(\lambda), \bar{y}(\lambda)$ , and  $\bar{z}(\lambda)$  are the tristimulus functions. The reflectance value,  $R(\lambda)$ , has been explicitly denoted as a function of the wavelength of the light. Substituting  $R(\lambda)$ , using Eq. 9, one can further express the tristimuli as

$$\begin{aligned} X &= X_{MD} - \Delta X \\ Y &= Y_{MD} - \Delta Y \\ Z &= Z_{MD} - \Delta Z \end{aligned} \quad (18)$$

where  $X_{MD}, Y_{MD}$  and  $Z_{MD}$  are the tristimulus values computed according to the Murray–Davies assumption and  $\Delta X, \Delta Y, \Delta Z$  are the contribution from light scattering or optical dot gain. Their expressions are, for example,

$$\begin{aligned} X_{MD} &= \int R_{MD}(\lambda)S(\lambda)\bar{x}(\lambda)d\lambda \\ \Delta X &= \int \Delta R(\lambda)S(\lambda)\bar{x}(\lambda)d\lambda \end{aligned} \quad (19)$$

If the tristimuli of the unprinted paper are  $(X_0, Y_0, Z_0)$ , due to the non-negativity of  $\Delta X$ ,  $\Delta Y$  and  $\Delta Z$ , there are the following inequalities:

$$\begin{aligned} X_0 - X &\geq X_0 - X_{MD} \\ Y_0 - Y &\geq Y_0 - Y_{MD} \\ Z_0 - Z &\geq Z_0 - Z_{MD} \end{aligned} \quad (20)$$

Therefore the present model predicts more saturated color than does the Murray–Davies assumption. This is actually the chromatic consequence of light scattering or the Yule–Nielsen effect.

### Summary

We present a model to simulate the multichromatic tone reproduction, which allows us to analyze properties of images printed with any number of inks and in any halftone scheme. By applying Gaussian type of point spread function (PSF) the Yule–Nielsen effect has been simulated for images printed with 2 inks and different dot geometries (round dots and square dots). The Yule–Nielsen effect shows a strong dependence on the optical properties of the substrate and ink, and on the geometric distributions of printed dots (shape, size, location and relative orientation of the dots). The present model is independent of the halftone scheme, and therefore it is applicable to images produced with any kind of halftone algorithm. 

**Acknowledgment.** This work was supported by the Surface Science and Printing Program of the Swedish Foundation for Strategic Research and the research program T2F.

### References

1. J. A. C. Yule and W. J. Nielsen, The penetration of light into paper and its effect on halftone reproduction, *TAGA Proc.* **3**, 65 (1951).
2. A. Murray, Monochrome reproduction in photoengraving, *J. Franklin Inst.* **221**, 721 (1936).
3. I. Pobboravsky and M. Person, Computation of dot areas required to match a colorimetrically specified color using the modified neugebauer equations, *TAGA Proc.*, 65 (1972).
4. F. R. Ruckdeschel and O. G. Hauser, Yule–Nielsen effect in printing: a physical analysis, *Appl. Opt.* **17**, 3376 (1978).
5. S. Gustavson, Dot Gain in Color Halftones, Ph.D. Dissertation No. 492,1997, Dept. of Electrical Engineering, Linköping University, Sweden.
6. S. Gustavson, Color gamut of halftone reproduction, *J. Imaging. Sci. Technol.* **41**, 283 (1997).
7. G. L. Rogers, Optical dot gain in a halftone print, *J. Imaging. Sci. Technol.* **41**, 643 (1997).
8. G. L. Rogers, Effect of light scatter on halftone color, *J. Opt. Soc. Amer. A* **15**, 1813 (1998).
9. G. L. Rogers, Neugebauer revisited: random dots in halftone screening, *Color Res. Appl.* **23**, 104 (1998).
10. G. L. Rogers, Optical dot gain: lateral scattering probabilities, *J. Imaging. Sci. Technol.* **42**, 341 (1998).
11. J. S. Arney, A probability description of the Yule–Nielsen effect, I, *J. Imaging. Sci. Technol.* **41**, 633 (1997).
12. J. S. Arney and M. Katsube, A probability description of the Yule–Nielsen effect II: The impact of halftone geometry, *J. Imaging. Sci. Technol.* **41**, 637 (1997).
13. J. R. Huntsman, A new model of dot gain and its application to a multilayer color proof, *J. Imaging. Technol.* **13**, 136 (1987).
14. L. Yang, R. Lenz, and B. Kruse, Light scattering and ink penetration effects on tone reproduction, *J. Opt. Soc. Amer. A* **18**,360 (2001).
15. Li Yang, Björn Kruse and Nils Pauler, A new model for ink penetration in tone reproduction (to be published).
16. J. A. C. Yule, D. J. Howe and J. H. Altman, *TAPPI Proc.* **50**, 337 (1967).
17. R. Saito and H. Kotera, Dot allocations in dither matrix with wide color gamut, *J. Imaging. Sci. Technol.* **43**, 345 (1999).